Efficient anomalous reflection through near-field interactions in metasurfaces

H. Chalabi, Y. Ra'di, D. L. Sounas, and A. Alù

Phys. Rev. B **96**, 075432 — Published 22 August 2017

DOI: 10.1103/PhysRevB.96.075432

Efficient anomalous reflection through near-field interactions in metasurfaces

H. Chalabi, Y. Ra'di, D. L. Sounas, and A. Alù

Department of Electrical and Computer Engineering, The University of Texas at Austin, Austin, TX 78712, USA

*To whom correspondence should be addressed: alu@mail.utexas.edu

Gradient metasurfaces have been extensively used in the past few years for advanced wave manipulation over a thin surface. These metasurfaces have been mostly designed based on the generalized laws of reflection and refraction. However, it was recently revealed that metasurfaces based on this approach tend to suffer from inefficiencies and complex design requirements. We have recently proposed a different approach to the problem of efficient beam steering using a surface, based on bianisotropic particles in a periodic array. Here, we show highly efficient reflective metasurfaces formed by pairs of isotropic dielectric rods, which can offer asymmetrical scattering of normally incident beams with unitary efficiency. Our theory shows that moderately broadband anomalous reflection can be achieved with suitably designed periodic arrays of isotropic nanoparticles. We also demonstrate practical designs using TiO2 cylindrical nanorods to deflect normally incident light towards a desired direction. The proposed structures may pave the way to a broader range of light management opportunities, with applications in energy harvesting, signaling and communications.

I. Introduction

Metamaterials are ensembles of carefully designed nanostructures that can be used to obtain special optical responses, such as negative refraction [1]-[3], subwavelength imaging [4] or cloaking [5]-[6]. Metamaterials in their three-dimensional form suffer from losses degrading their performance and challenges in their realization, especially as the wavelength shrinks and the inclusions have to become extremely small. Metasurfaces on the other hand are more immune to losses and can be realized with lithographic approaches, and therefore have attracted significant attention [7]-[12].

These surfaces can be realized for the purpose of beam shaping in the form of gradient metasurfaces, which offer the possibility of realizing a wide range of electromagnetic and optical functionalities [13]-[23]. So far, the approaches taken for the design of such metasurfaces consist predominantly in engineering the local reflection coefficient or the impedance, leading to graded impedance profiles [13]. This technique requires the realization of a gradually inhomogeneous profile for the metasurface properties, usually spanning over a wide range of values, which may require fine discretization in order to implement it in practice. It may also imply going through resonances for the involved elements, which enhances losses and does not enable a uniform amplitude distribution as the phase changes. The necessity to discretize these continuous phase profiles also leads to the necessity of small constituent elements. Another problem with the local design approach is that it is limited by a fundamental upper bound regarding the power that can be transmitted in a particular direction [24]-[26], as long as we consider passive elements forming the surface, which decreases as the difference between incident and transmitted directions increases.

In this work, we focus on metasurfaces for the purpose of asymmetrical scattering of normally incident light. This is a challenging task to do using gradient metasurfaces based on the generalized law of reflection and refraction where the efficiency dramatically drops when the steering angle increases (e.g., see [14]). These structures are important for applications such as filters [27], lenses [28] and sensors [29]. Moreover, they can be used for trapping of normally incident light inside a slab for the purpose of increased absorption efficiency. Therefore, these surfaces may become important for improving the performance of many devices, such as photodetectors and solar cells [30]-[32]. Moreover, such scatterers can be used for frequency-dependent steering of the impinging light, which may be useful for LIDAR systems [33], efficient signaling and tagging.

Recently the concept of meta-grating was proposed, based on which, it was shown that a periodic array of individual bianisotropic particles enables asymmetric scattering of a normally incident wave to a desired direction [34]. In addition to unitary efficiency, this concept eliminates the need for gradient impedance profiles that require high-resolution discretization of metasurfaces. Here we show that this response can be synthesized using a pair of isotropic particles in each unit cell of a metasurface. Our proposed technique does not pose a limitation on the minimum size of the metasurface particles, and therefore it relaxes fabrication requirements, without restricting the available wavefront transformation functionalities or compromising the efficiency. A similar approach was recently taken to realize a focusing lens, however the proposed design does not provide unitary efficiency [28].

In this paper, we start by investigating the details of the near-field interaction between resonant dipoles positioned on top of a perfect electric conductor, assuming that the dipoles are made of polarizable materials. By specifically considering the components of different

diffraction orders in the far-field, we obtain some relationships that should hold to obtain an asymmetric reflection profile of choice. Finally, we present practical designs for metasurfaces steering normally incident light to steep angles based on the presented theoretical analysis.

II. Theoretical analysis

We consider a periodic array of polarizable elements over a reflecting ground plane, tailored to achieve efficient asymmetrical reflection, which is of importance in wavefront transformation operations using a thin metasurface [25]. Let us first consider a two-dimensional (2D) array of dipoles, $\mathbf{p} = p_z \hat{z}$, at angular frequency ω located at height d on top of a perfect electric conductor. The electric field radiated by the array is given by [35]

$$E_{sca} = \frac{-j\mu\omega^2}{4} p_z \left(\sum_{n=-\infty}^{\infty} H_0^{(2)} \left(k\sqrt{\rho_n^2 - 2\rho_n d \sin(\theta_n) + d^2} \right) - \sum_{n=-\infty}^{\infty} H_0^{(2)} \left(k\sqrt{\rho_n^2 + 2\rho_n d \sin(\theta_n) + d^2} \right) \right). \quad (1)$$

In this equation, $\rho_n = \sqrt{(x-nP)^2 + y^2}$ and $\theta_n = \tan^{-1}(y/(x-nP))$ and the two terms in parenthesis correspond to radiation from the dipoles and their images. Moreover, μ corresponds to the vacuum permeability and $H_0^{(2)}$ refers to the zero order Hankel function of the second kind. It can be verified that having a single resonant dipole per unit cell is not sufficient to achieve asymmetrical reflection for normal incidence, consistent with the fact that a symmetric array cannot steer the beam from normal to one oblique direction suppressing the scattering towards the opposite direction. In Appendix A, we show however that two dipoles per unit cell with suitably tailored asymmetric phase difference in their respective polarizability is sufficient to realize beam steering from normal incidence to an oblique direction with unitary efficiency. In

our theoretical analysis, we assume two polarizable dipoles per unit cell, induced by the incoming incident wave.

In order to steer the wave to the desired angle θ (see geometry in Fig. 1), the array periodicity should satisfy the Bragg's condition $P = \lambda / \cos(\theta)$. We are interested in the case for which only three diffraction orders exist, corresponding to left, normal and right outgoing waves. This condition can be satisfied if $\theta < \pi / 3$. Let us consider now two dipoles with out of plane moments p_{z1} and p_{z2}, laterally separated by the distance l and positioned at heights d_1 and d_2 from the ground plane. In this scenario, it is possible to obtain the radiated electric field based on an analysis similar to the diffraction order analysis presented in [35] and outlined in Appendix A

$$\begin{aligned} E_{ff} = & \frac{\mu\omega^2}{P}\left[p_{z1}\sin(k_t d_1) + p_{z2}\sin(k_t d_2) e^{j2\pi\frac{l}{P}} \right] \frac{e^{-j2\pi\frac{x}{P} - jk_t y}}{k_t} \\ & + \frac{\mu\omega^2}{P}\left[p_{z1}\sin(k_t d_1) + p_{z2}\sin(k_t d_2) e^{-j2\pi\frac{l}{P}} \right] \frac{e^{j2\pi\frac{x}{P} - jk_t y}}{k_t} \\ & + \frac{\mu\omega^2}{Pk}\left[p_{z1}\sin(kd_1) + p_{z2}\sin(kd_2) \right] e^{-jky}. \end{aligned} \quad (2)$$

where $k_t = \sqrt{k^2 - \left(\frac{2\pi}{P}\right)^2}$. Since, we want to reflect the incoming light towards one direction, the power that goes to the other diffraction order should be cancelled. This criterion puts a constraint on the polarizabilities required for the two dipole moments. The corresponding details for the specific case $d_1 = d_2 = d$ are provided in Appendix A. After some algebraic manipulation, we obtain the required static polarizabilities

$$\frac{1}{\alpha_{p1,ll}}=\frac{\mu\omega^2}{4\sin\left(2\pi\frac{l}{P}\right)}\Im\left\{e^{-j2\pi l/P}j\left(\sum H_0^{(2)}\left(2\pi\sqrt{\frac{\left(n-\frac{l}{P}\right)^2}{\cos^2\left(\theta_{defl.}\right)}+\left(\frac{2d}{\lambda}\right)^2}\right)-\sum H_0^{(2)}\left(\frac{2\pi\left|n-\frac{l}{P}\right|}{\cos\left(\theta_{defl.}\right)}\right)\right)\right.$$
$$+j\sum H_0^{(2)}\left(2\pi\sqrt{\frac{\left(n+\frac{l}{P}\right)^2}{\cos^2\left(\theta_{defl.}\right)}+\left(\frac{2d}{\lambda}\right)^2}\right)-j\sum H_0^{(2)}\left(\frac{2\pi\left|n+\frac{l}{P}\right|}{\cos\left(\theta_{defl.}\right)}\right)$$
$$\left.+\left(j+je^{-j2\pi l/P}\right)\left(1+\sum_{n\neq 0}H_0^{(2)}\left(\frac{2\pi|n|}{\cos\left(\theta_{defl.}\right)}\right)-\sum H_0^{(2)}\left(2\pi\sqrt{\frac{n^2}{\cos^2\left(\theta_{defl.}\right)}+\left(\frac{2d}{\lambda}\right)^2}\right)\right)\right\}$$

and

$$\frac{1}{\alpha_{p2,ll}}=\frac{-\mu\omega^2}{4\sin\left(2\pi\frac{l}{P}\right)}\Im\left\{e^{j2\pi l/P}j\left(\sum H_0^{(2)}\left(2\pi\sqrt{\frac{\left(n+\frac{l}{P}\right)^2}{\cos^2\left(\theta_{defl.}\right)}+\left(\frac{2d}{\lambda}\right)^2}\right)-\sum H_0^{(2)}\left(\frac{2\pi\left|n+\frac{l}{P}\right|}{\cos\left(\theta_{defl.}\right)}\right)\right)\right.$$
$$+j\sum H_0^{(2)}\left(2\pi\sqrt{\frac{\left(n-\frac{l}{P}\right)^2}{\cos^2\left(\theta_{defl.}\right)}+\left(\frac{2d}{\lambda}\right)^2}\right)-j\sum H_0^{(2)}\left(\frac{2\pi\left|n-\frac{l}{P}\right|}{\cos\left(\theta_{defl.}\right)}\right)$$
$$\left.+\left(j+je^{j2\pi l/P}\right)\left(1+\sum_{n\neq 0}H_0^{(2)}\left(\frac{2\pi|n|}{\cos\left(\theta_{defl.}\right)}\right)-\sum H_0^{(2)}\left(2\pi\sqrt{\frac{n^2}{\cos^2\left(\theta_{defl.}\right)}+\left(\frac{2d}{\lambda}\right)^2}\right)\right)\right\}.$$

The previous expressions do not include radiation loss, therefore the dynamic polarizabilities are given by $\alpha=\left(\alpha_{p1,2ll}{}^{-1}+j\frac{k^2}{4}\right)^{-1}$. This condition on the required polarizabilities depends on a given height and separation of dipoles, and it allows totally suppressing the power carried by the left diffraction order. After having suppressed the power going to this channel, we should cancel the power that is specularly reflected. Assuming that Eqs. (3) and (4) are satisfied, the ratio of

power going to the anomalous diffraction order versus the incident power can be calculated in closed form:

$$\frac{P_R}{P_{inc}} = \frac{16}{\pi^2}\frac{\sin^2\left(2\pi\frac{d}{\lambda}\sin(\theta)\right)\sin^2\left(2\pi\frac{d}{\lambda}\right)\cos^2(\theta)}{\sin(\theta)} \times\left|\frac{\mu\omega^2\alpha_{p1}}{4}\left(\frac{g_2-\kappa_2}{g_1g_2-\kappa_1\kappa_2}\right)+\frac{\mu\omega^2\alpha_{p2}}{4}\left(\frac{g_1-\kappa_1}{g_1g_2-\kappa_1\kappa_2}\right)e^{j2\pi\frac{l}{P}}\right|^2, \tag{5}$$

with uniteless quantities $g_{1,2}$ and $\kappa_{1,2}$ given by

$$\begin{aligned} g_1 &= 1+\frac{j\mu\omega^2}{4}\alpha_{p1}\left(\sum_{n\neq 0}H_0^{(2)}\left(k|nP|\right)-\sum H_0^{(2)}\left(k\sqrt{n^2P^2+4d^2}\right)\right), \\ g_2 &= 1+\frac{j\mu\omega^2}{4}\alpha_{p2}\left(\sum_{n\neq 0}H_0^{(2)}\left(k|nP|\right)-\sum H_0^{(2)}\left(k\sqrt{n^2P^2+4d^2}\right)\right), \\ \kappa_1 &= \frac{j\mu\omega^2}{4}\alpha_{p1}\left(\sum H_0^{(2)}\left(k|nP-l|\right)-\sum H_0^{(2)}\left(k\sqrt{(nP-l)^2+4d^2}\right)\right), \\ \kappa_2 &= \frac{j\mu\omega^2}{4}\alpha_{p2}\left(\sum H_0^{(2)}\left(k|nP+l|\right)-\sum H_0^{(2)}\left(k\sqrt{(nP+l)^2+4d^2}\right)\right). \end{aligned} \tag{6}$$

Based on this formula, we can calculate the achievable efficiency for asymmetrical scattering for a given height and separation between dipoles [leading to determined polarizabilities α_1 and α_2 based on Eqs. (3) and (4)], and choose these parameters to maximize the coupling to the anomalous diffraction order. By investigating Eq. (5), it is possible to realize unitary efficiency for a desired deflection angle.

We can use cylinders with appropriate refractive indices in order to realize the necessary polarizabilities required for the asymmetrical scattering [see Fig. 1]. The required polarizabilities can be implemented using cylinders with the same specific radius. The refractive index needed for a cylinder with radius r is obtained with the formula, derived in Appendix A,

$$n^2 - 1 = \frac{(P/r)^2}{\pi^3} \frac{\cos^2(\theta)}{\alpha_{ll}^{-1} - 0.049 - \frac{1}{\pi} log\left(\left(\frac{r}{P}\right)^2 \frac{\pi^2}{\cos^2(\theta)}\right)}. \quad (7)$$

Using this equation we can calculate the required refractive indices in order to achieve the required polarizabilities.

III. Realistic design made of TiO_2 cylinders

Since it is difficult to find materials with a specific refractive index at the frequency of interest, we can instead use cylinders with different radius sizes, but an available refractive index to achieve the required polarizabilities. Aiming to address the wavelength of 700 nm and knowing that the relative permittivity of TiO_2 is 5.1 at this wavelength, we can obtain the size of cylinders needed for the asymmetrical scattering. The design parameters and achieved efficiencies for different scattering angles have been listed in Table 1. Based on these fine-tuned radii, the ratio of scattered power to different diffraction orders is calculated over a range of frequencies for the three considered scattering angles. The corresponding results are shown in Fig. 2.

Fabricating structures in which the required resonators are located at a specific height from the ground plane may be difficult in practice. To address this problem, we also consider structures in which the required cylinders are located right above the substrate. Using the same lateral distances between the cylinders as those used before, we find through optimization the required sizes. The necessary radii of cylinders for different scattering angles in these modified designs are summarized in Table 2. Moreover, in order to investigate the sensitivity of the designs to the fabrication errors, we have calculated the efficiencies for the structures with the radius of

cylinders deviated ±5% from the optimal designs. These efficiencies have been listed in Table 2. The corresponding frequency responses and field distributions of such designs are shown in Fig. 3. We have also investigated the effect of the incidence angle variation in the efficiency of these designs. Based on our calculations the efficiency does not become lower than 91.6%, 93.5%, and 92.2% for incidence angles between -5 to +5 degrees for deflection angles of 30, 35 and 45 degrees, respectively. It should be noted that the proposed structures provide a reasonably wide bandwidth, despite being based on resonant particles. The reason behind this response is that the size of the particles is not necessarily significantly subwavelength, given that the period is not small compared to the wavelength and that we use only two particles per period to control the scattering.

IV. **Conclusions**

In this paper, we have derived the conditions to realize efficient anomalous reflection with an optical metasurface consisting of periodic arrays of pairs of rods. The derived conditions require the rods to be near their resonance frequencies, and in this scenario the near-field interaction between the two elements allow ideally engineering the far-field response. Based on a thorough theoretical analysis, we have investigated the potential designs providing high efficiency for different deflection angles. The proposed designs consist of dielectric cylinders on top of a reflective ground plane, providing the possibility of achieving nearly 100% efficient asymmetrical scattering. These designs overcome the obstacles arising in similar designs based on gradient metasurfaces, as they do not need lossy and active regions to reach comparable efficiencies. Moreover, they relax the necessity of fine discretization and the requirement of having several small elements per unit cell. Furthermore, fabricating the proposed designs may

be achieved with conventional lithographic techniques. The analysis presented here can be extended to structures that support more than three diffractive channels in the far-field by using more than two dielectric rods, providing exciting opportunities for further control of the scattering and radiation in the far-field based on tuning the near-field interaction between resonators. The proposed structures can be used for different applications in energy harvesting and holography.

Acknowledgements

This work was supported by the Department of Defense, the National Science Foundation and the Welch Foundation with grant No. F-1802.

Appendix A

- **Radiation fields of a periodic array of pairs of dipoles located over a ground plane**

The total radiation fields of two adjacent dipoles $\mathbf{p}_1 = p_{z1}\hat{z}$ and $\mathbf{p}_2 = p_{z2}\hat{z}$ located over a ground plane can be written as

$$E_{tot} = \omega^2 \mu \sqrt{\frac{1}{2\pi k\rho}} e^{j\frac{\pi}{4}} e^{-jk\rho} \sin\left(kd\sin(\theta)\right)\left(p_{z1} + p_{z2}e^{-jks\cos(\theta)}\right)\hat{z}. \quad (8)$$

This function suggests that it is possible to get zero emission in a specific direction by tuning different parameters. For an array located over a ground plane, the total contribution can be obtained through the superposition

$$
\begin{aligned}
E_{sca} = & \frac{-j\mu\omega^2}{4} p_{z,1}\left(\sum_{n=-\infty}^{\infty} H_0^{(2)}\left(k\sqrt{\rho_{n,1}^2 - 2\rho_{n,1}d_1\sin\left(\theta_{n,1}\right)+d_1^2}\right)\right) \\
& + \frac{-j\mu\omega^2}{4} p_{z,1}\left(-\sum_{n=-\infty}^{\infty} H_0^{(2)}\left(k\sqrt{\rho_{n,1}^2 + 2\rho_{n,1}d_1\sin\left(\theta_{n,1}\right)+d_1^2}\right)\right) \\
& + \frac{-j\mu\omega^2}{4} p_{z,2}\left(\sum_{n=-\infty}^{\infty} H_0^{(2)}\left(k\sqrt{\rho_{n,2}^2 - 2\rho_{n,1}d_2\sin\left(\theta_{n,2}\right)+d_2^2}\right)\right) \\
& + \frac{-j\mu\omega^2}{4} p_{z,2}\left(-\sum_{n=-\infty}^{\infty} H_0^{(2)}\left(k\sqrt{\rho_{n,2}^2 + 2\rho_{n,2}d_2\sin\left(\theta_{n,2}\right)+d_2^2}\right)\right).
\end{aligned} \tag{9}
$$

In this equation, $\rho_{n,1} = \sqrt{\left(x - nP\right)^2 + y^2}$, $\theta_{n,1} = \tan^{-1}\left(y/\left(x - nP\right)\right)$, $\rho_{n,2} = \sqrt{\left(x - nP - l\right)^2 + y^2}$, and $\theta_{n,2} = \tan^{-1}\left(y/\left(x - nP - l\right)\right)$. The local electric fields at the location of two dipoles ($y = d_1$ and $x = 0$ as well as $y = d_2$ and $x = l$) are given by

$$
\begin{aligned}
E_{z,loc1} = & E_{z,ext1} - \frac{j\mu\omega^2}{4} p_{z,1}\left(\sum_{n\neq 0} H_0^{(2)}\left(k\left|nP\right|\right) - \sum H_0^{(2)}\left(k\sqrt{n^2P^2 + 4d_1^2}\right)\right) \\
& - \frac{j\mu\omega^2}{4} p_{z,2}\left(\sum H_0^{(2)}\left(k\sqrt{\left(nP + l\right)^2 + \left(d_2 - d_1\right)^2}\right) - \sum H_0^{(2)}\left(k\sqrt{\left(nP + l\right)^2 + \left(d_2 + d_1\right)^2}\right)\right), \\
E_{z,loc2} = & E_{z,ext2} - \frac{j\mu\omega^2}{4} p_{z,2}\left(\sum_{n\neq 0} H_0^{(2)}\left(k\left|nP\right|\right) - \sum H_0^{(2)}\left(k\sqrt{n^2P^2 + 4d_2^2}\right)\right) \\
& - \frac{j\mu\omega^2}{4} p_{z,1}\left(\sum H_0^{(2)}\left(k\sqrt{\left(nP - l\right)^2 + \left(d_2 - d_1\right)^2}\right) - \sum H_0^{(2)}\left(k\sqrt{\left(nP - l\right)^2 + \left(d_2 + d_1\right)^2}\right)\right).
\end{aligned}
$$

Moreover, the total far-field radiation can be written as in Eq. (2). If p_{z1} and p_{z2} be in-phase, then if the left going power be zero then the right going wave will also be zero. However, if there exist a phase delay between them as Δ then

$$
\left|p_{z1}\right|\sin\left(k_t d_1\right) + \left|p_{z2}\right|\sin\left(k_t d_2\right)e^{j\left(\Delta - \frac{2\pi l}{P}\right)} = 0. \tag{11}
$$

Such a phase difference can be induced by the difference between the external electric field and the local one. Moreover, since we want the normally outgoing wave to be zero, therefore

$$
\frac{\mu\omega^2}{Pk}\left(p_{z1}\sin\left(kd_1\right) + p_{z2}\sin\left(kd_2\right)\right)e^{-jky} = E_0 e^{-jky}. \tag{12}
$$

However it is possible to have

$$\left|p_{z1}\right|\sin\left(k_t d_1\right)+\left|p_{z2}\right|\sin\left(k_t d_2\right)e^{j\left(\Delta+\frac{2\pi l}{P}\right)}\neq 0. \tag{13}$$

It can be shown that

$$\begin{aligned} E_{z,loc1} &= \left(\frac{g_2 E_{z,ext1}-\kappa_2 E_{z,ext2}}{g_1 g_2-\kappa_1\kappa_2}\right), \\ E_{z,loc2} &= \left(\frac{g_1 E_{z,ext2}-\kappa_1 E_{z,ext1}}{g_1 g_2-\kappa_1\kappa_2}\right), \end{aligned} \tag{14}$$

where

$$\begin{aligned} g_1 &= 1+\frac{j\mu\omega^2}{4}\alpha_{p1}\left(\sum_{n\neq 0}H_0^{(2)}\left(k\left|nP\right|\right)-\sum H_0^{(2)}\left(k\sqrt{n^2P^2+4d_1^2}\right)\right), \\ g_2 &= 1+\frac{j\mu\omega^2}{4}\alpha_{p2}\left(\sum_{n\neq 0}H_0^{(2)}\left(k\left|nP\right|\right)-\sum H_0^{(2)}\left(k\sqrt{n^2P^2+4d_2^2}\right)\right), \\ \kappa_1 &= \frac{j\mu\omega^2}{4}\alpha_{p1}\left(\sum H_0^{(2)}\left(k\sqrt{\left(nP-l\right)^2+\left(d_2-d_1\right)^2}\right)-\sum H_0^{(2)}\left(k\sqrt{\left(nP-l\right)^2+\left(d_2+d_1\right)^2}\right)\right), \\ \kappa_2 &= \frac{j\mu\omega^2}{4}\alpha_{p2}\left(\sum H_0^{(2)}\left(k\sqrt{\left(nP+l\right)^2+\left(d_2-d_1\right)^2}\right)-\sum H_0^{(2)}\left(k\sqrt{\left(nP+l\right)^2+\left(d_2+d_1\right)^2}\right)\right). \end{aligned} \tag{15}$$

After some algebraic manipulation, assuming that $d_1 = d_2$, we can obtain the static polarizabilities as in Eqs. (3) and (4). These are the required polarizabilities for a given height and separation to eliminate the power carried by the left diffraction order. Having removed the power going to this channel, it remains to consider the power that back scatters normally. If the incident field be given as $E_0 e^{jk_0 y}$ then the diffraction orders will have the following relative amplitudes:

$$\begin{aligned} \frac{E_R}{E_0} &= \frac{4j\sin\left(2\pi\frac{d}{\lambda}\sin\left(\theta\right)\right)}{\pi\sin\left(\theta\right)}\frac{\sin\left(2\pi\frac{d}{\lambda}\right)\cos\left(\theta\right)}{g_1 g_2-\kappa_1\kappa_2} \\ &\left(\frac{\mu\omega^2\alpha_{p1}}{4}\left(g_2-\kappa_2\right)+\frac{\mu\omega^2\alpha_{p2}}{4}\left(g_1-\kappa_1\right)e^{j2\pi\frac{l}{P}}\right)e^{-j2\pi\frac{x}{P}-j\sqrt{k^2-\left(\frac{2\pi}{P}\right)^2}y}, \end{aligned} \tag{16}$$

which corresponds to the power ratio in Eq. (5).

- **Scattering of normally incident light from a cylinder**

Since we are interested here in the scattering of an incident wave with electric field parallel to the axis, we write the electric field as $E = E_z\hat{z} = u\hat{z}$. Then, the wave equation becomes $\nabla^2 u + n(r)^2 k^2 u = 0$, where $n(r) = 1$ in the air and $n(r) = n$ in the cylinder. Assuming that the incident field is a plane wave, $u = E_0 e^{-jkr\cos(\varphi)}$, and applying proper boundary conditions we get two required conditions at $r = a$:

$$\begin{aligned} J_m'(ka) - b_m H_m'(ka) &= n d_m J_m'(nka), \\ J_m(ka) - b_m H_m(ka) &= d_m J_m(nka), \end{aligned} \tag{17}$$

where

$$b_m = \frac{nJ_m'(nka)J_m(ka) - J_m'(ka)J_m(nka)}{nJ_m'(nka)H_m(ka) - H_m'(ka)J_m(nka)}.$$

Knowing that the electric field of a dipole with moment of p is given by $E = \frac{-\omega\mu(j\omega p_z)}{4} H_0^{(2)}(k\rho)\hat{z}$, the following equation holds for the polarizability of the cylinder

$$\alpha = \frac{p_z}{E_0} = \frac{4N}{j\omega^2 \mu D},$$

where

$$N = -\frac{1}{2}(n^2 - 1)x + O(x^3),$$

$$D = \frac{2j}{\pi x} - \frac{1}{2}(n^2 - 1)x\left(1 - \frac{j}{\pi}\left(log\left(\frac{x^2}{4}\right) + 2\gamma - 1\right)\right) + O(x^3),$$

Here e is the Euler–Mascheroni constant. This equation results in the condition between refractive index and the required polarizabilities [see Eq. (7)].

References

[1] D. R. Smith, J. B. Pendry, and M. C. K. Wiltshire, *Metamaterials and Negative Refractive Index*," Science 305, 788 (2004).

[2] R. A. Shelby, D. R. Smith, and S. Schultz, *Experimental Verification of a Negative Index of Refraction*, Science 292, 77 (2001).

[3] V. M. Shalaev, *Optical negative-index metamaterials*, Nat. Photonics 1, 41 (2007).

[4] Z. Liu, H. Lee, Y. Xiong, C. Sun, and X. Zhang, *Far-Field Optical Hyperlens Magnifying Sub-Diffraction-Limited Objects*, Science 315, 1686 (2007).

[5] A. Alù and N. Engheta, *Achieving Transparency with Plasmonic and Metamaterial Coatings*, Phys. Rev. E 72, 016623 (2005).

[6] D. Schurig, J. J. Mock, B. J. Justice, S. A. Cummer, J. B. Pendry, A. F. Starr, and D. R. Smith, *Metamaterial Electromagnetic Cloak at Microwave Frequencies*, Science 314, 977 (2006).

[7] C. L. Holloway, E. F. Kuester, J. A. Gordon, J. O'Hara, J. Booth, and D. R. Smith, *An Overview of the Theory and Applications of Metasurfaces: The Two-Dimensional Equivalents of Metamaterials*, IEEE Antennas Propag. Mag. 54, 10 (2012).

[8] C. Pfeiffer and A. Grbic, *Metamaterial Huygens' Surfaces: Tailoring Wave Fronts with Reflectionless Sheets*, Phys. Rev. Lett. 110, 197401 (2013).

[9] A. V. Kildishev, A. Boltasseva, and V. M. Shalaev, *Planar Photonics with Metasurfaces*, Science 339, 1232009 (2013).

[10] Y. Zhao, X. -X. Liu, and A. Alù, *Recent Advances on Optical Metasurfaces*, J. Opt. 16, 123001 (2014).

[11] N. Yu and F. Capasso, *Flat Optics with Designer Metasurfaces*, Nat. Mater. 13, 139 (2014).

[12] S. B. Glybovski, S. A. Tretyakov, P. A. Belov, Y. S. Kivshar, and C. R. Simovski, *Metasurfaces: From Microwaves to Visible*, Phys. Rep. 634, 1 (2016).

[13] N. Yu, P. Genevet, M. A. Kats, F. Aieta, J.-P. Tetienne, F. Capasso, and Z. Gaburro, *Light Propagation with Phase Discontinuities: Generalized Laws of Reflection and Refraction*, Science 334, 333 (2011).

[14] S. Sun, K.-Y. Yang, C.-M. Wang, T.-K. Juan, W. T. Chen, C. Y. Liao, Q. He, S. Xiao, W.-T. Kung, G.-Y. Guo, L. Zhou, and D. P. Tsai, *High-Efficiency Broadband Anomalous Reflection by Gradient Meta-Surfaces*, Nano Lett. 12, 6223 (2012).

[15] A. Pors, M. G. Nielsen, R. L. Eriksen, and S. I. Bozhevolnyi, *Broadband Focusing Flat Mirrors Based on Plasmonic Gradient Metasurfaces*, Nano Lett. 13, 829 (2013).

[16] M. Esfandyarpour, E. C. Garnett, Y. Cui, M. D. McGehee, and M. L. Brongersma, *Metamaterial Mirrors in Optoelectronic Devices*, Nat. Nanotechnol. 9, 542 (2014).

[17] M. Kim, A. M. H. Wong, and G. V. Eleftheriades, *Optical Huygens Metasurfaces with Independent Control of the Magnitude and Phase of the Local Reflection Coefficients*, Phys. Rev. X 4, 041042 (2014).

[18] F. Monticone, N. Mohammadi Estakhri, and A. Alù, *Full Control of Nanoscale Optical Transmission with a Composite Metascreen*, Phys. Rev. Lett. 110, 203903 (2013).

[19] N. Mohammadi Estakhri, V. Neder, M. W. Knight, A. Polman, and A. Alù, *Visible Light, Wide-Angle Graded Metasurface for Back Reflection*, ACS Photon. 4, 228 (2017).

[20] N. Mohammadi Estakhri, and A. Alù, *Recent Progress in Gradient Metasurfaces*, J. Opt. Soc. Am. B 33, A21 (2015).

[21] N. Mohammadi Estakhri, C. Argyropoulos, and A. Alù, *Graded Metascreens to Enable a New Degree of Nanoscale Light Management*, Phil. Trans. A 373, 20140351 (2015).

[22] Z. Bomzon, G. Biener, V. Kleiner, and E. Hasman, *Space-Variant Pancharatnam–Berry Phase Optical Elements with Computer-Generated Subwavelength Gratings*, Opt. Lett. 27, 1141 (2002).

[23] V. S. Asadchy, Y. Ra'di, J. Vehmas, and S. A. Tretyakov, *Functional Metamirros Using Bianisotropic Elements*, Phys. Rev. Lett. 114, 095503 (2015).

[24] N. Mohammadi Estakhri, and A. Alù, *Wavefront Transformation with Gradient Metasurfaces*, Phys. Rev. X 6, 041008 (2016).

[25] V. S. Asadchy, M. Albooyeh, S. N. Tcvetkova, A. Díaz-Rubio, Y. Ra'di, and S. A. Tretyakov, *Perfect Control of Reflection and Refraction Using Spatially Dispersive Metasurfaces*, Phys. Rev. B 94, 075142 (2016).

[26] A. Epstein and G. V. Eleftheriades, *Huygens' Metasurfaces via the Equivalence Principle: Design and Applications*, JOSA B 33, A31 (2016).

[27] W. Suh and S. Fan, *All-Pass Transmission or Flattop Reflection Filters Using a Single Photonic Crystal Slab*, Appl. Phys. Lett. 84, 4905 (2004).

[28] R. Paniagua-Dominguez, Y. F. Yu, E. Khaidarov, R. M. Bakker, X. Liang, Y. H. Fu, and A. I. Kuznetsov, *A Metalens with Near-Unity Numerical Aperture*, arXiv: 1705.00895 [physics.optics].

[29] E. Chow, A. Grot, L. W. Mirkarimi, M. Sigalas, and G. Girolami, Ultracompact Biochemical Sensor Built with Two-Dimensional Photonic Crystal Microcavity, Opt. Lett. 29, 1093 (2004).

[30] F. Xia, T. Mueller, Y. -M. Lin, A. Valdes-Garcia, and P. Avouris, *Ultrafast Graphene Photodetector*, Nat. Nanotechnol. 4, 839 (2009).

[31] Z. Yu, A. Raman, and S. Fan, *Fundamental Limit of Nanophotonic Light Trapping in Solar Cells*, Proc. Natl. Acad. Sci. 107, 17491 (2010).

[32] A. Pospischil, M. M. Furchi, and T. Mueller, *Solar-Energy Conversion and Light Emission in an Atomic Monolayer p–n Diode*, Nat. Nanotechnol. 9, 257 (2014).

[33] A. Yaacobi, J. Sun, M. Moresco, G. Leake, D. Coolbaugh, and M. R. Watts, *Integrated Phased Array for Wide-Angle Beam Steering*, Opt. Lett. 39, 4575 (2014).

[34] Y. Ra'di, D. L. Sounas, and A. Alù, *Metagratings: Beyond the Limits of Graded Metasurfaces for Wavefront Control*, arXiv: 1705.03879 [physics.optics].

[35] S. Tretyakov, *Analytical Modeling in Applied Electromagnetics electromagnetics* (Artech House, Norwood, MA, 2003)**.**

Figures

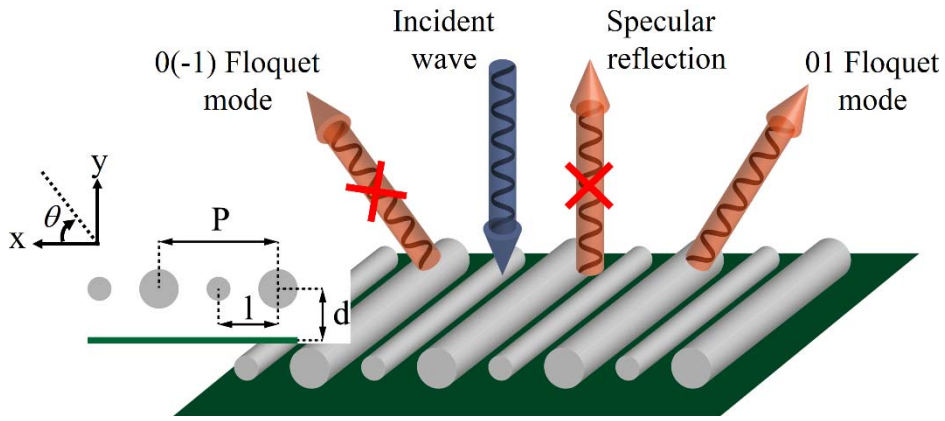

Fig. 1. Schematic of the geometry under analysis.

Table 1. Design parameters for an array of cylinders located at a certain distance from the ground plane

					Exact radii from analytical derivations			Radii after a fine optimization		
Scattering angle (deg)	d/λ	l/P	$\alpha_{ll,1}$	$\alpha_{ll,2}$	r_1	r_2	Efficiency (%)	r_1	r_2	Efficiency (%)
30	0.15	0.26	0.911877	5.28068	P / 18.9	P / 12.6	93	P / 18	P / 11	97.5
35	0.15	0.27	0.910905	7.03184	P / 19.9	P / 12.8	93	P / 19	P / 10.6	96.5
45	0.15	0.29	0.963991	10.5506	P / 22.7	P / 14.1	89	P / 21.2	P / 11.3	94

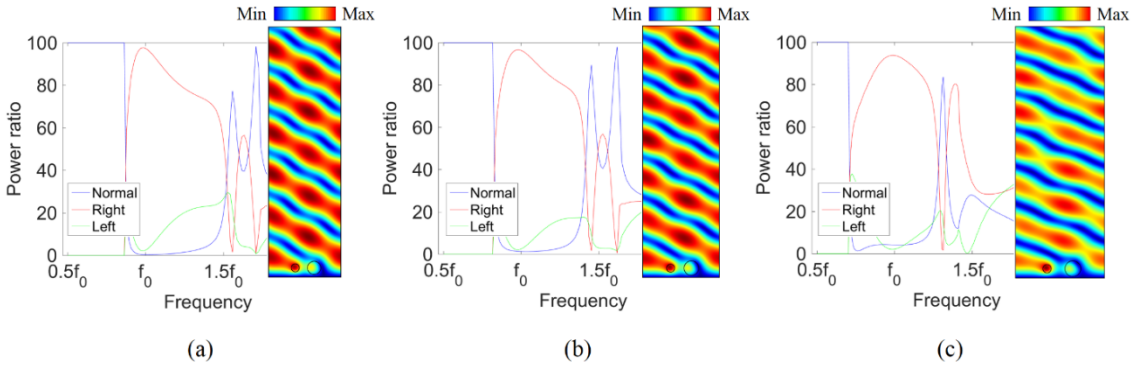

Figure 2: Frequency variation of the scattered power to different diffraction orders for the TiO_2 cylinders located at the same height from the ground plane for deflection angles of (a) 30 deg (b) 35 deg (c) 45 deg.

Subsets in these plots show the numerical simulations for the normalized electric fields for frequencies with maximum efficiency.

Table 2. Design parameters for an array of TiO_2 cylinders located right on top of the ground plane

Scattering angle (deg)	r_1	r_2	Efficiency (%)	Efficiency (%) For the design with +5% error	Efficiency (%) For the design with -5% error
30	P / 13.6	P / 9.3	96.5	93.3	88.3
35	P / 14.1	P / 9.8	97.1	92.9	92.0
45	P / 15.7	P / 11.2	94.3	89.1	92.9

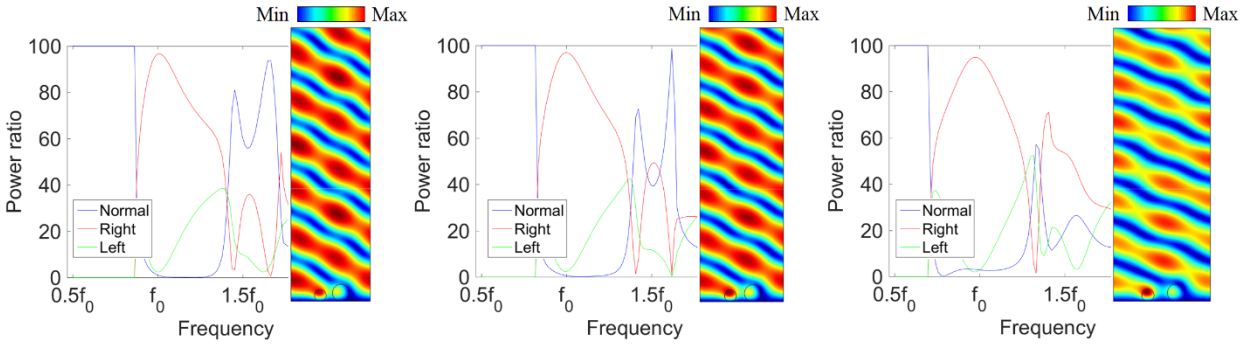

Figure 3: Frequency variation of the scattered power to different diffraction orders for practical TiO_2 cylinders located right on top of the ground plane for deflection angles of (a) 30 deg (b) 35 deg (c) 45 deg. Subsets in these plots show the numerical simulations for the normalized electric fields for frequencies with maximum efficiency.